ELSEVIER

Progress in Organic Coatings 40 (2000) 139–150

PROGRESS IN ORGANIC COATINGS

www.elsevier.com/locate/porgcoat

Structure and properties of multiphase particles and their impact on the performance of architectural coatings

B. Schuler [a,*], R. Baumstark [b], S. Kirsch [a], A. Pfau [a], M. Sandor [a], A. Zosel [a]

[a] *BASF AG, Polymer Laboratory, D-67056 Ludwigshafen, Germany*
[b] *BASF AG, Marketing Coatings Raw Materials, D-67056 Ludwigshafen, Germany*

Abstract

Aqueous dispersions used as binders in low-pigmented solvent-free paint formulations have to cope with the challenge to simultaneously guarantee an excellent film formation and appearance as well as good block resistance and hardness. One strategy to fulfill these contradictory requirements is the employment of multiphase particles.

In this work it is proved that the structure of latex particles, synthesized by a two-stage emulsion polymerization process, can be correlated to the morphology and properties of the dispersion films as well as to the application properties of the corresponding paint films.

Two sets of model dispersions were made. In the first set, the hard/soft ratio was varied, in the second set the amount of the AA. The structure of the particles was determined by TEM, and a morphology map was derived. AFM demonstrated a clear correlation between the particle structure and the morphology of the latex film. Dynamic mechanical analyses verified the presence of two distinct polymers with the hard phase acting as a transparent filler. For the hard/soft series, the properties of the dispersion films such as block resistance, gloss and hardness could be attributed to their structure. A closer look on the block behavior revealed that it can be related to the tack and surface roughness of the dispersion film, but not to its internal strength. Solvent free emulsion gloss paints were formulated, and application tests performed. The properties of the paint films correlated very well with those of the dispersion films. The test results clearly show that dispersions of multiphase particles enable the formulation of solvent free paints with excellent film-forming ability in combination with high block resistance, hardness and gloss.

Abbreviations: AA, acrylic acid; AFM, atomic force microscopy; *n*BA, *n*-butyl acrylate; BDG, butyl diglycol; MMA, methyl methacrylate; MFFT, minimum film formation temperature; PVC, pigment volume concentration; PMMA, poly-methyl methacrylate; P*n*BA, poly-*n*-butyl acrylate; pbw, parts by weight; pphm, parts per hundred monomers; TEM, transmission electron microscopy; T_g, glass transition temperature

Keywords: Multiphase particles; Particle structure; Solvent free paints; Morphology; AFM

1. Introduction

The different application fields of aqueous dispersions often require the latex to fulfill contradictory requirements. Binders for architectural coatings, e.g. wood coatings or emulsion gloss paints, have to cope with the demand for simultaneously allowing a smooth film formation, and showing a high block resistance and film hardness. A neat film can be achieved with a paint containing a binder with a low minimum film formation temperature (MFFT); a high block resistance and hardness on the other hand can be adjusted by employing a polymer binder with high T_g. In traditional paints, using a hard polymer binder and a coalescent solves this problem. The coalescent decreases the MFFT to a level desired for perfect film formation. After the application of the paint to a substrate, the coalescent evaporates and the hard polymer remains. Due to increasing environmental awareness, a clear trend can be identified towards paints with low amounts of volatile organic compounds (VOCs) [1–3]. Therefore, new strategies were considered to combine the contradictory requirements in latex binders.

One solution to the problem is the blending of two dispersions of different MFFT: the low MFFT dispersion as the film forming species and the high MFFT dispersion to impart block resistance [4]. Winnik and Feng [5] reported that in order to gain transparent films, the hard latex has to be sufficiently small, the mixing ratio has to be optimized, and the refractive index of the two components has to be comparable.

The effect of the size and volume ratio of the hard and soft particles on the film structure was described in terms of the percolation theory by Eckersley and Helmer [6]. If the

* Corresponding author.

0300-9440/00/$ – see front matter
PII: S0300-9440(00)00136-3

particle size ratio R_{soft}/R_{hard} is sufficiently large, the block resistance of a mixture is improved because of the hard particles forming a network. In addition, it was detected that the fine hard particles tend to accumulate on the film surface.

A more convenient approach to the problem, however, are multiphase particles. Two or more different polymers are simultaneously present in one latex particle. One important advantage of this technique is that there is a very homogenous distribution of the phases throughout the polymer film [7], especially if, through grafting reactions, the different polymers are covalently fixed to each other, considerably reducing the tendency of phase separation [8]. In addition, the manufacturing of a hard small latex ($\ll$100 nm) as a mixing compound requires larger amounts of water-soluble raw materials like emulsifiers or functional monomers for stabilization, leading to an increased water sensitivity of the final blend. From the industrial point of view, storing and mixing of dispersions requires additional investment at the production site.

One of the most important processes to manufacture multiphase particles is semi-batch emulsion polymerization [9]. When it is run under starved conditions, the amount of unconverted monomers is kept low in comparison to the already formed polymer, and a change in the composition of the monomer feed results in an almost immediate generation of the second phase polymer. For the (meth)acrylates considered in this work, the starved conditions are easy to achieve because they show an instantaneous conversion of more than 95% under standard conditions of polymerization.

In order to obtain a well-defined latex, it is important to prevent the system from forming second-generation particles. This implies that the polymerization process needs to be optimized with regard to the number of species being able to induce new particles by a micellar mechanism or secondary homogenous nucleation, including emulsifiers, initiator and water-soluble monomers like unsaturated carboxylic acids.

The structure of the multiphase particles is influenced by thermodynamic and kinetic factors. The basis for the thermodynamic analysis of multiphase particles was given by Torza and Mason [10] who examined the interfacial behavior of three mutually immiscible fluids and found, depending on the interfacial tension of the different phases, structures like complete engulfing, partial engulfing or nonengulfing. These considerations were transferred to the description of multiphase particles by Sundberg et al. [11,12]. They calculated the Gibbs's free energy of multiphase particles by the equation

$$G = \sum \gamma_{ij} A_{ij}$$

with γ being the interfacial tension between the different polymer phases and water, respectively, and A being the contact area of the phases i and j.

This concept was taken further by El-Aasser et al. [13], who developed a mathematical model to describe free energy differences between different possible particle structures, and thus allowed the determination of the thermodynamically most favorable structure of a given system.

The interfacial energy between two phases can be influenced by a large variety of parameters. Important factors are monomer composition, emulsifier and initiator. Experimental results reported by several authors were summarized by Rudin and Lee [14,15].

In many multistage emulsion polymers, the expected equilibrium structures could not be found. Instead, thermodynamically unstable phase distributions were detected. Okubo, for example, reported structures which he designated "raspberry-like", "confetti-like", "snowman-like", "octopus-like" or "mushroom-like" [16]. Cho and Lee obtained particles that displayed a "sandwich-like" arrangement [17]. Those nonequilibrium structures could impart unexpected film properties. Zhao et al. [18] described particles with hard microdomains embedded in a soft matrix dramatically increasing tensile strength and the elongation of the corresponding film.

Considerations and calculations were conducted by Winzor and Sundberg [19], like why the final thermodynamic equilibrium cannot be reached. During the polymerization, the dominance of a single equilibrium morphology may not be likely due to a constant change in the phase ratio and the influence of the monomer on the interfacial tensions of the different phases. The competition between phase separation and polymerization kinetics can lead to the existence of a range of occluded morphologies differing only little in energy. These small differences combined with high local viscosity of the polymerizing phase would then prevent the coalescence of the occlusions to yield the fully phase separated morphology.

Factors that affect the local viscosity and hence the mobility of the polymer chains are, for example,

1. polymerization temperature,
2. crosslinking,
3. grafting,
4. addition rate of monomers.

In the work presented here, a systematic approach was taken to correlate the structures of multiphase particles to those of their films and then, based on the structures, to understand the mechanical behavior of the latex films as well as the application properties of corresponding emulsion gloss paints. Therefore, a set of dispersions was made where the soft/hard ratio was varied from 100/0 to 0/100. The soft phase consisted of a polymer with the composition 65.7% *n*BA, 32.8% MMA and 1.5% AA (T_g: -4°C), and the hard phase of 98.5% MMA and 1.5% AA (T_g: $+105^\circ$C) (Table 1).

Additionally, a second set of dispersions was synthesized where the soft/hard ratio was kept constant at 75/25, but the amount of the AA was varied. In this series, the soft phase consisted solely of P*n*BA, the hard phase of PMMA. This series was conceived to study the influence of AA, that is important for lattices of industrial relevance, on the morphology of the particles and the films (Table 2).

Table 1
Composition and characteristics of the dispersions and the corresponding films: set 1[a]

Sample	Phase 1 (mass %)	Phase 2 (mass %)	Particle size (nm)	MFFT[b] (°C)	Pendulum hardness[c] (s)	Film gloss[d] 20°/60°	Water uptake[e] (%)
S 100–0	100	0	115	<0	4	70/82	18
S 85–15	85	15	116	<0	14	71/84	19
S 75–25	75	25	107	<0	28	73/84	12
S 70–30	70	30	106	<0	32	74/84	9
S 65–35	65	35	123	6	39	73/83	11
S 60–40	60	40	123	10	46	64/82	14
S 50–50	50	50	111	>40	No film formation at 25°C		6
S 40–60	40	60	114	>40	No film formation at 25°C		8
S 25–75	25	75	118	>40	No film formation at 25°C		
S 0–100	0	100	83	>40	No film formation at 25°C		

[a] Phase 1: 65.7% *n*BA/32.8% MMA/1.5% AA; phase 2: 98.5% MMA/1.5% AA.
[b] According to ISO 2115 plastics.
[c] 200 μm film (wet), 24 h drying time, according to DIN 53157.
[d] 200 μm film (wet), 24 h drying time, measured with a Byk Gardener Micro-TRI-Gloss meter.
[e] With 2% BDG (S 50–50, S 40–60 with 10%), 7 days drying time (25°C/50% humidity), according to DIN 53495.

2. Experimental

2.1. Synthesis of the lattices

The lattices were prepared by a standard semi-batch emulsion polymerization process employing a constant amount of sodium dodecylsulfate (SDS) (2.25 pphm) as emulsifier and sodium persulfate (0.25 pphm) as initiator. The polymerization was carried out at 85°C. The emulsion feed time was 3 h. The feed rate was kept constant throughout the polymerization. At the end, the dispersions were neutralized by addition of sodium hydroxide. The solids content was adjusted to 45 wt.%.

2.2. Particle size measurement

The particle size distribution was determined by means of an analytical ultracentrifuge. All of the lattices showed a monomodal particle size distribution. No indication of a second generation of particles could be found.

2.3. Transmission electron micrographs

The samples were subjected to ultrafiltration prior to the TEM examination to remove water-soluble compounds that reduce the contrast between the different phases. The dispersions were then treated with a 2 wt.% aqueous solution of uranyl acetate (UAc) as a negative stain. It surrounds the particles, and thus improves the contrast by staining the background light gray. Additionally, it prevents the particles from touching and possibly forming a film. After deposition on a copper grid, the samples were treated with ruthenium tetroxide vapor (RuO_4) as a preferential stain for the *n*BA containing soft polymer phase.

Table 2
Composition and characteristics of the dispersions: set 2[a]

Sample	AA phase 1 (mass %)	AA phase 2 (mass %)	Particle size (nm)	MFFT[b] (°C)
A 0–0	0	0	118	<0
A 0.75–0.75	0.75	0.75	108	<0
A 1.9–1.9	1.9	1.9	123	<0
A 3–3	3	3	140	<0

[a] Phase 1 (75%): P*n*BA; phase 2 (25%): PMMA.
[b] According to ISO 2115 plastics.

2.4. Atomic force microscopy (AFM)

All AFM data presented here were recorded in Tapping Mode using Si cantilevers (35 N/m, ν_0 approximately 300 kHz, Nanoprobe). The Tapping Mode can be used to map distributions of different materials (e.g. soft and hard materials can be distinguished). Details of the method and the evaluation are published elsewhere [20].

RMS-roughness is calculated as

$$R_{\mathrm{rms}} = \frac{1}{L_x L_y}\left(\iint (z_i - z_{\mathrm{ave}})^2 \,\mathrm{d}x\,\mathrm{d}y\right)^{1/2}$$

$(z_i - z_{\mathrm{ave}})$ is the distance of the actual height of the measured point (z_i) to the best fit plane of the surface at the same (x, y). $L_x L_y$ is the scanned area.

2.5. Dynamic mechanical analysis

Free films were formed by casting the dispersions on silicon moulds, from which the film could be removed after drying at room temperature. The dynamic Youngs's modulus E^* of samples from these films were measured with a frequency of 1 Hz. E^* consists of two components, the storage modulus E' and the loss modulus E''. They were plotted on a logarithmic scale versus temperature.

2.6. Tensile testing

Test specimens were prepared according to DIN 53455. Tensile tests were performed at 23°C and 50% relative humidity with an Instron tensile tester. The crosshead speed was 20 mm/min, the gauge length 22 mm.

2.7. Tack

The tackiness of the film surfaces was studied with an instrument of the probe tack test with a flat-ended probe which has been developed in our laboratory a few years ago, and about which more details are published elsewhere [21]. It measures the energy of separation of the probe from the film surface under defined conditions of contact formation and separation. This energy is a measure for the tack of the film.

2.8. Block testing

The dispersions and formulated paint were drawn down on a support and dried for 24 h. Two defined areas of the film were brought in contact. The specimens were loaded with a weight and kept at a given temperature for a certain time (the exact conditions are given in the corresponding tables). At room temperature, the samples were separated and the block behavior was judged with marks:

0 no tack, test samples fall apart;
1 very slight tack, test samples can be separated easily;
2 slight tack;
3 moderate tack, small areas are pulled out;
4 very tacky, larger areas are pulled out;
5 no separation possible.

3. Results and discussion

3.1. Single particles

The first part deals with the dependence of the particle structure on the phase ratio and the amount and distribution of the AA. TEM is a powerful technique to characterize the morphology of multiphase particles. Single particles can be observed directly, and detailed information about the structures and surface properties of the latex particles can be obtained. The necessary contrast between the different phases has to be induced by using special staining techniques [22,23] (see Section 2).

For the series with the soft/hard ratio being varied, the TEM-pictures indicate that with low amounts of the hard PMMA-phase (S 85–15) no structure could be detected, and the particles looked more or less like those consisting of pure soft phase (S 100–0). This is due to the fact that the particles are still too soft and the negative stain does not sufficiently prevent the particles from flattening. As a consequence, the particles seem to be approximately twice as large as measured by the analytical ultracentrifuge. With the reduced layer thickness, the electron density decreases and subsequently the resolution becomes too low to detect the hard phase. However, the AFM results (see Section 3.2) indirectly prove the presence of an independent hard phase. The situation changes when the amount of the hard phase is increased. For the S 75–25 sample (and this is also true for S 70–30), a PMMA "bump" structure could be resolved (Fig. 1). The particles are nonspherical, and the light-gray colored PMMA phase is sitting in patches on the darker gray soft phase. By further increasing the share of the hard phase to 35 and 40% (S 65–35 and S 60–40), the particles become more spherical and the hard-phase material forms a continuous cover over the soft phase. It is still visible as broad cracks on the surface of the final particles. By increasing the amount of the hard phase to 50% (S 50–50), the shell is further closing. Only very small patches of the soft phase can be detected. At higher hard/soft ratios, the soft phase is no longer visible and a perfect core/shell particle is formed.

In the second set of experiments, the soft to hard ratio was kept constant (75 BA/25 MMA), and the amount and phase distribution of the AA was varied as indicated in Table 2. The structure of these particles is especially interesting because unsaturated acids play an important role in the stabilization of dispersions in industrial production processes. The high polarity of the AA should change the surface tension and, therefore, the compatibility of the different polymers. The TEM pictures of the samples A 0–0 (not containing any AA) and A 1.9–1.9 (with 1.9% of AA being present in both phases) prove that changes in the AA content indeed strongly influence the particle morphology. A 0–0 represents a nonspherical acorn-like structure. The P*n*BA phase is slightly stained and can be easily distinguished from the MMA phase. In contrast, the A 1.9–1.9 particles look more spherical, but the PMMA phase now forms several microdomains (Fig. 1).

In Fig. 2, all the structures of the samples according to TEM pictures are schematically summarized in a morphology map. The particles of the S-series show an increasing engulfment of the soft phase up to the formation of a core/shell structure with an increasing hard/soft ratio. The structures observed represent the thermodynamic equilibrium calculated according to the concept that the system adjusts the minimum overall surface tension [11–13]. In contrast to the S-series, only the sample free of AA reaches the thermodynamic equilibrium in the A-series. Copolymerization of AA leads to an increasing tendency of the particles to contain microdomains. The system is obviously increasingly governed by kinetic factors. The reason might be that during polymerization the second phase initially forms small microdomains in the existing particles due to different places of entry of the active radical species. The thermodynamic equilibrium is reached through diffusion and coalescence. With increasing amount of AA, the mobility of the polymer chains could possibly be reduced because of increasing

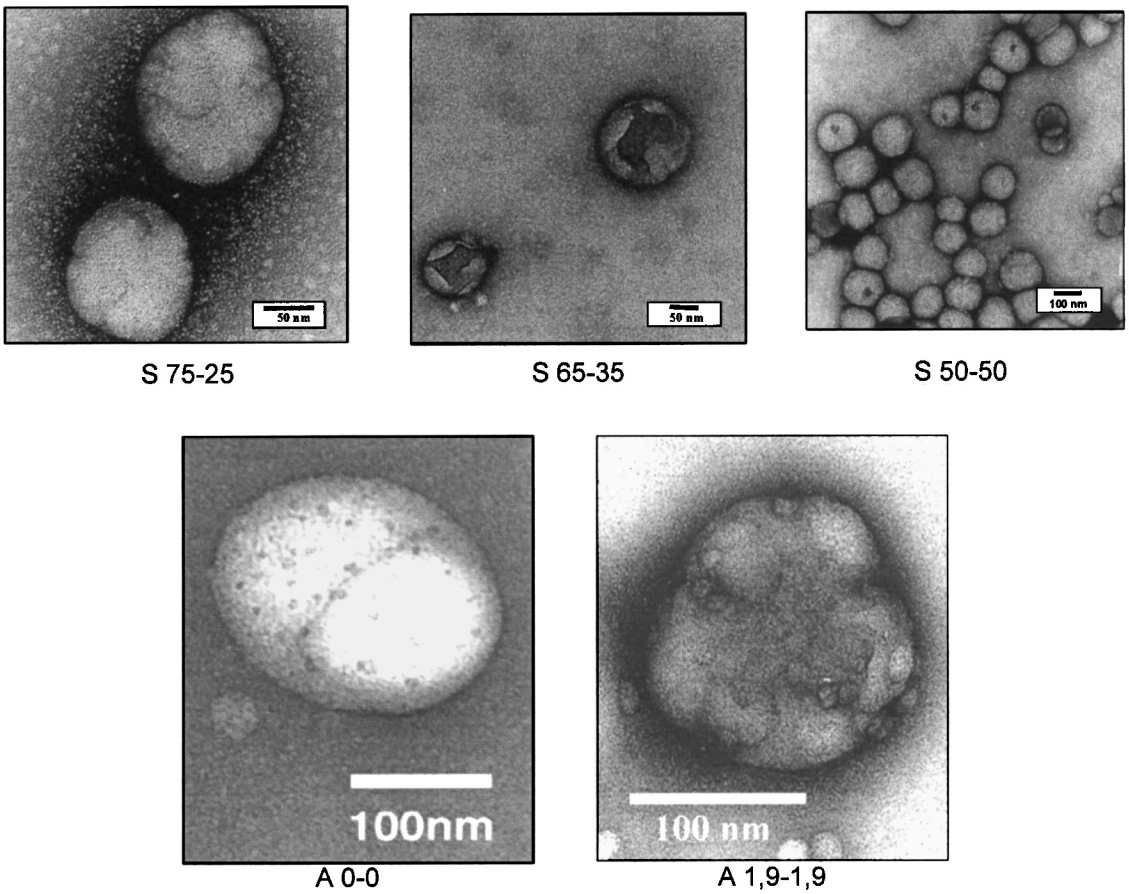

Fig. 1. TEM pictures of latex particles with different soft/hard phase ratios and AA contents.

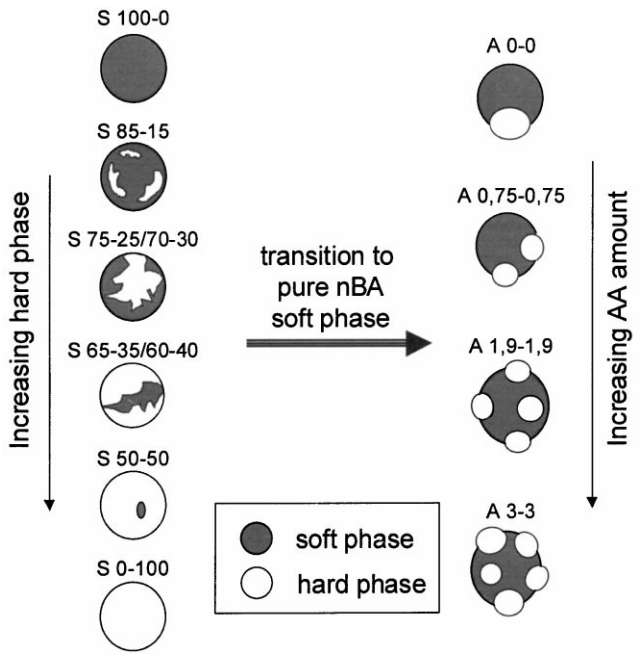

Fig. 2. Morphology map of the structured particles examined according to TEM.

facilities of hydrogen bond formation. This leads to the microdomain structure being preserved.

3.2. Latex film

3.2.1. Atomic force microscopy (AFM)

The most crucial question to be asked when looking at the structure of the single particles is whether the structure is preserved during film formation. If this is so, the film structure can be tailored by control of the polymerization process.

AFM is a powerful tool to obtain detailed information about the structure of the polymer film. The nondestructive Tapping Mode combined with phase imaging allows the user to distinguish between materials of different mechanical behavior on a nm-scale. In the case of the samples examined here, the soft phase can be differentiated from the hard phase.

In Fig. 3, the results are given for the samples S 85–15, S 75–25, S 65–35 and S 50–50. The film structures clearly match the TEM results. The increasing engulfment of the soft phase is seen easily. The S 85–15 film can be interpreted in terms of PMMA patches distributed in the soft phase matrix, whereas in the S 75–25 and S 65–35 film “half-moon” like structures increasingly dominate the film. The fact that the hard phase seems to show different shapes is due to

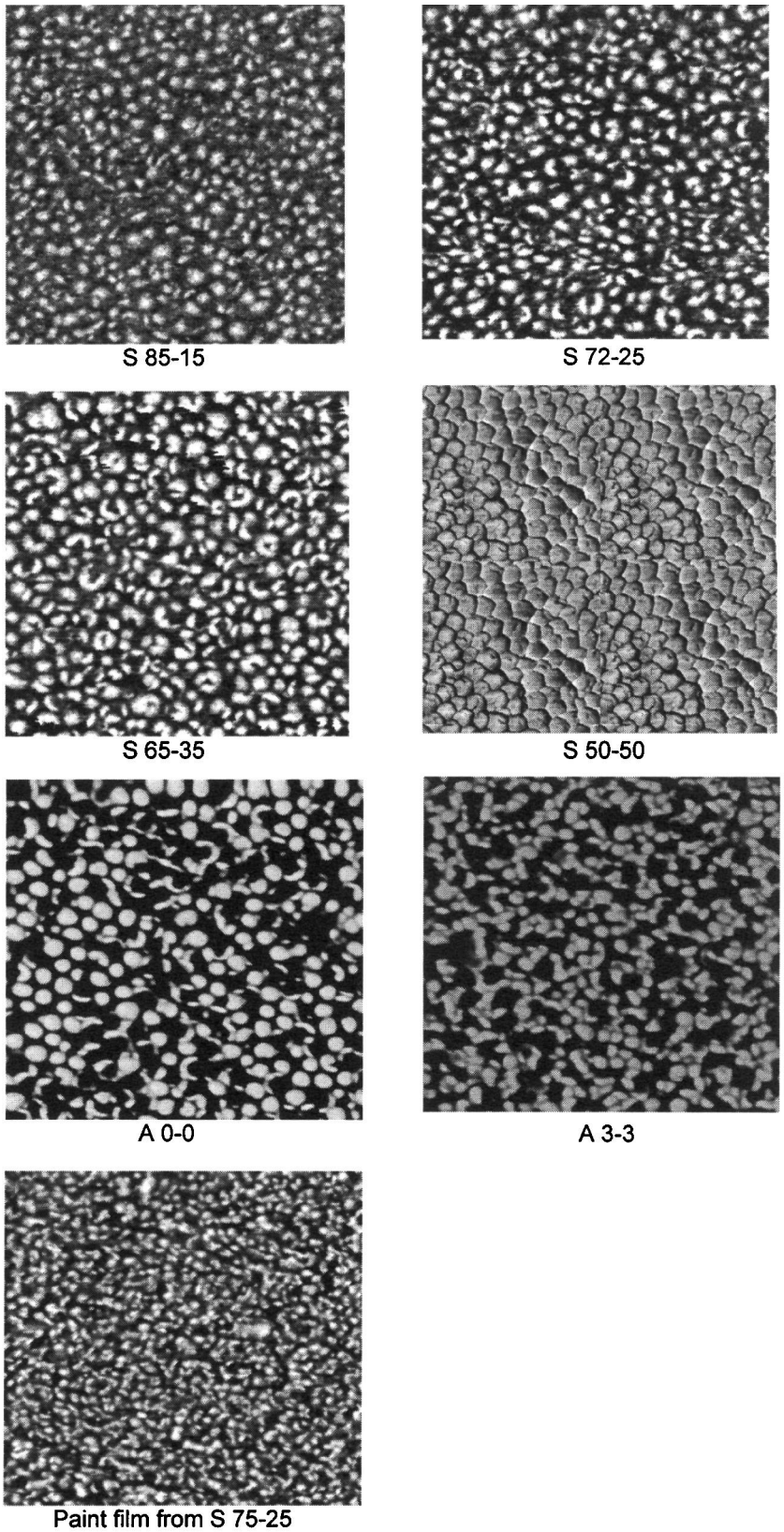

Fig. 3. AFM pictures (2 μm × 2 μm) of dispersion films of samples with different soft/hard phase ratios and different AA contents. Also included is one example of a paint film formulated with S 75–25.

the particles being randomly oriented. As a consequence, the AFM images views from different angles of the same structure. S 50–50, that forms no film at room temperature, displays slightly deformed single particles. The soft phase material could not be detected anymore. Another important statement can be derived from the AFM pictures. They do not indicate any tendency of the hard phase to aggregate and form lumps which is well known for blends of hard and soft lattices [5–7]. The phases are well distributed throughout the film. There is no danger that through different drying conditions the film structure changes.

In the AA series, the AFM pictures of the samples A 0–0 and A 3–3 are in perfect accordance with the TEM, too (Fig. 3). For A 0–0, the "acorn-like" structure can readily be identified, whereas in the A 3–3 sample small domains of hard particles are present.

In conclusion, the AFM results demonstrate that the structure of the single particles is maintained during film formation, and that it determines the film structure. Thus, through goal-directed utilization of the kinetic and thermodynamic parameters during the syntheses of multiphase particles, a large variety of different structures are accessible. In comparison to blends that are restricted to spherical particles, this higher degree of freedom enables to tailor the morphology of the dispersion film as desired.

Knowing the latex film structure, the question arises whether it can be correlated to its properties. Therefore, MFFT, pendulum hardness, gloss, block resistance and water uptake were measured. Additionally, the films were characterized by their dynamic mechanical properties, stress/strain behavior and tack.

3.2.2. MFFT, pendulum hardness, gloss and water uptake

The MFFT of the films of the S-series (Table 1) correlates to the structures obtained by TEM and AFM. As long as the film is governed by the soft phase (S 100–0 to S 70–30) the MFFT stays below 0°C. With the hard phase increasingly engulfing the soft phase, the film is dominated by the nonfilm-forming hard phase, and the MFFT increases significantly. S 50–50 does not forms a film at room temperature. The particles come into contact through the high-MFFT hard phase which shields the soft areas. Due to the increasing presence of the hard phase at the surface of the film, the pendulum hardness steadily increases. The gloss measurements at angles of 20 and 60° indicate that as long as a film is formed the gloss of the latex film stays unchanged. Only S 60–40 displays slightly reduced gloss at 20°. This might be a consequence of hindered film formation. The water uptake surprisingly varies little with the phase ratio, despite the fact that with a higher share of the more hydrophilic hard phase an increase was expected, and there is even a tendency in the opposite direction.

3.2.3. Mechanical characteristics

Films of multiphase particles can be studied by dynamic mechanical analyses (DMA) yielding, e.g., the dynamic modulus as a function of the temperature. Conclusions can be drawn from the modulus versus temperature plots on the existence of two glass transition ranges, and their position and extension on the temperature scale [24]. However, neither the phase ratio nor further information about the structure of the particles can be derived from the *E*-moduli curves.

3.2.3.1. Increasing share of the hard phase (S-series). The E'-moduli versus temperature plots of the samples S 100–0 to S 50–50 clearly show two different glass transition ranges of the composite particles (Fig. 4). The BA/MMA copolymer, which is polymerized in the first stage, has a glass transition temperature of −4°C for all samples. The glass

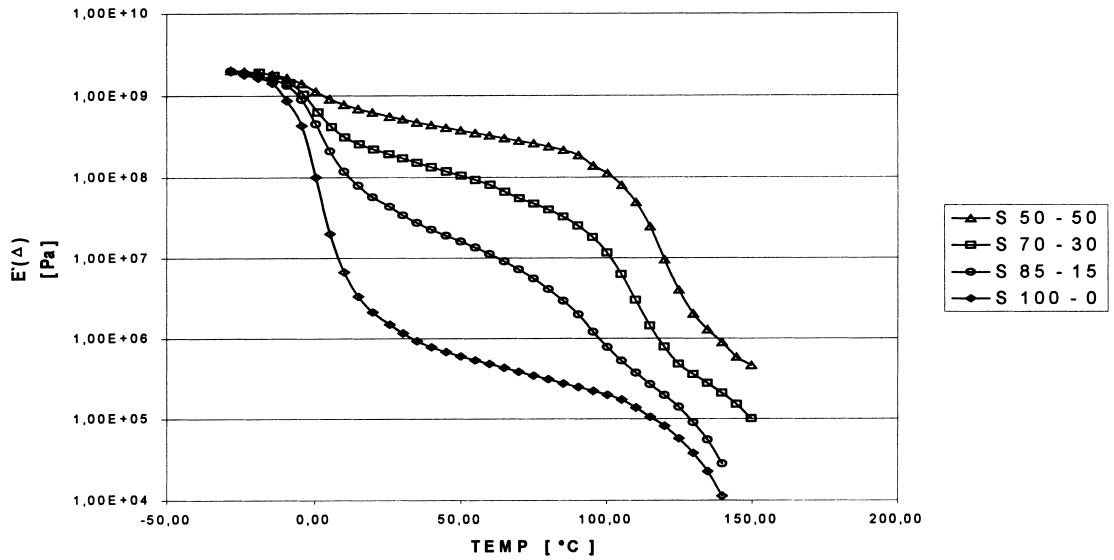

Fig. 4. E'-moduli vs. temperature for different soft/hard ratios.

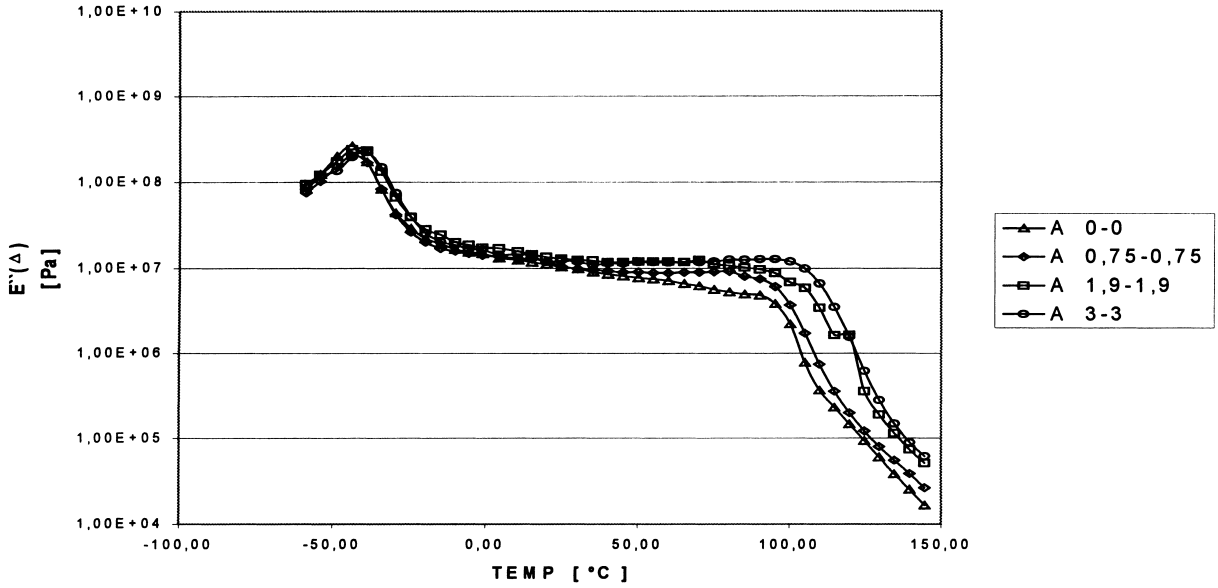

Fig. 5. E''-moduli vs. temperature for different AA contents.

transition range of PMMA which is formed in the second stage is apparent as a distinct decrease of the moduli above about 100°C for the samples with 50 and 30% of the second stage polymer. The material containing only 15% shows a gradual decrease of E' above the glass transition range of the soft phase. In this case, the amount of the PMMA component apparently is too small to form a second phase with a separate glass transition range. On the whole, the moduli curves reveal that the PMMA phase acts as a hard transparent filler in the polymer film.

3.2.3.2. Variations of the amount of acrylic acid (A-series). The T_g's, determined by the maxima of the E''-curves, of the soft as well as of the hard polymer is shifted to higher values (Fig. 5). They fit quite well to the data calculated by the Fox-equation [25] (Table 3). Obviously, the predominant amount of the AA copolymerizes homogeneously with BA in the first and MMA in the second stage.

3.2.4. Block resistance

The block test can be considered as a very crude form of the peel test common in the adhesive industry. The resistance to peeling off of an adhesive is determined by measuring the force required either to peel off an adhesive strip from a rigid surface or to draw apart two substrates coated with the adhesive (T-peel test [26]). The latter method being closer to the block test. In the peel test, two modes of failure can be observed. One is the adhesive failure, where film separation takes place at the interface of the two surfaces in contact. No residue of the adhesive can be found on the surface it was peeled off from. In contrast, the cohesive fracture results in a failure of the bond inside the polymer, and the adhesive can be found on both surfaces being separated.

In analogy, the block test materials with a good performance show an adhesive failure. The surfaces can be separated easily and the integrity of the coating is preserved (block marks: 0–2). Coatings with a poor block behavior on the other hand tend to fail cohesively. Domains with increasing size are pulled out of the coating (marks: 3–4) until the composite cannot be separated at all without destroying the support (mark: 5).

The peel resistance of a polymer is a rather complex phenomenon and is influenced by several factors [27] which, therefore, should also be of importance for the block behavior. The following three essential factors will be examined closely for the dispersions under consideration.

1. Tack.
2. Surface roughness.
3. Internal strength (cohesion).

Table 3
Measured and calculated T_g's (°C) of the single polymer phases of the samples with different AA content

Sample	A 0–0	A 0.75–0.75	A 1.9–1.9	A 3–3
T_g calculated (BA-phase)	−43	−42	−40	−39
T_g measured (BA-phase)	−44	−43	−41	−39
T_g calculated (MMA-phase)	105	106	107	108
T_g measured (MMA-phase)	100	100	109	114

Table 4
Block test, tack measurement and E'-moduli of dispersion films with different hard/soft ratio

Sample	S 100–0	S 85–15	S 70–30	S 60–40	S 50–50
Block test[a]	5	3	1	0	0
Tack (80°C) (J/m^2)	16.6	4.9	1.2	0	0
E'-moduli (80°C) (Pa)	2.5×10^5	2.0×10^6	2.5×10^7	8.5×10^7	1.9×10^8

[a] 200 μm film (wet) on Leneta foil (24 h drying time), contact area: 2 cm × 2 cm, 80°C/24 h/500 g/cm^2.

3.2.4.1. Tack. If two surfaces are brought in contact with each other**,** interaction of the species at the surface takes place. These interactions can be merely van der Waals forces, but can also be of polar or even ionic nature. In the case of two surfaces coated with polymers, entanglement can take place additionally. Tack is defined as the property to form a connection of measurable strength to a substrate under usually slight pressure after short contact time [28]. At the first glance, the tack evaluation has only little in common with the block testing where comparably high loads are applied for long duration. But at the molecular level, the tack measurement gives insight into the mobility of the polymer chains on the surface of the polymer film. The higher the mobility of the chains, the easily they adhere to a surface brought in contact, and form a bond. During the block test, the mobile polymer molecules interdiffuse and bridge the interface. The forces necessary to tear apart the laminate are a consequence of this mechanism. Thus, the tack measurement should allow to qualitatively judge the strength of the connection at the interface.

The tack measurements of the latex films were performed at the same temperature at which the block testing was carried out (80°C). The results are given in Table 4. It is clearly demonstrated that the increase in the hard phase material at the film surface results in a reduced tack and in a corresponding improved block resistance.

The dependence of the tack on the phase ratio can also be derived from the E'-moduli measurements (Table 4). The E' values at 80°C, a temperature between the glass transition ranges of both phases, increase with the rising amount of the hard phase, as the moduli of both components contribute to the modulus of the film. Generally, the tack decreases with increasing modulus due to a decrease of the ability of the polymer to deform and form an intimate contact with the substrate. The agreement between the temperature dependence of E' and the block resistance of structured particles was also reported by Heuts et al. [29].

3.2.4.2. Surface roughness. Further explanation for the improvement of the block resistance can be derived from the AFM results if they are analyzed in terms of surface roughness. With an increasing amount of the hard phase, the film surface becomes more structured on the nano-scale (Table 5). This behavior can be interpreted in terms of the soft phase forming a continuous film and the rigid hard phase sticking out of it. The larger the hard phase species become, the higher the roughness of the film gets. Therefore, the contact area of the soft polymer is further reduced improving the block resistance. However, the importance of this effect in comparison to the tack cannot be judged.

3.2.4.3. Internal strength (cohesion). Tacky films can still be separated without being ruptured if the internal strength or cohesion is sufficiently high. The cohesive strength is usually measured by the so-called shear test [30]. An adhesive joint to a stainless steel plate is loaded with a weight. In this experimental setup, the adhesive joint usually breaks cohesively. The time it takes for the joint to fail is a measure of its cohesive strength. Unfortunately, this method cannot be applied to the polymers examined here. Because of their low tackiness at room temperature, they do not form a strong enough bond with the stainless steel plate and, therefore, under load fail by adhesive break. Thus, the standard shear test is unfit for estimating the cohesive strength of the samples.

Therefore, we decided to use stress/strain measurements to estimate the internal strength of the films. Table 6 lists the tensile strength σ_B and the elongation ε_B at break. With increasing amount of the hard phase material, the tensile strength increases and the elongation decreases. This behavior is typical for a soft polymer blended with a filler [31]. The area under the stress–strain curve represents the toughness or fracture energy of the film, measured in J/cm^3. It is the energy that has to be applied to destroy the film. If it stays below that value, the film is only stretched and

Table 5
Surface roughness of the dispersion films with different soft/hard ratio (1 μm × 1 μm area evaluated)

Sample	S 100–0	S 85–15	S 70–30	S 65–35	S 60–40
RMS-roughness (nm)	0.4	1.0	2.3	3.5	4.3

Table 6
Tensile strength σ_B and elongation ε_B at break and fracture energy E_f for dispersion films with different hard/soft ratio

Sample	σ_B (MPa)	ε_B (%)	E_f (J/cm^3)
S 100–0	0.6	2200	22.5
S 85–15	4.6	570	20.4
S 70–30	4.7	400	18.2
S 60–40	5.2	200	11.8

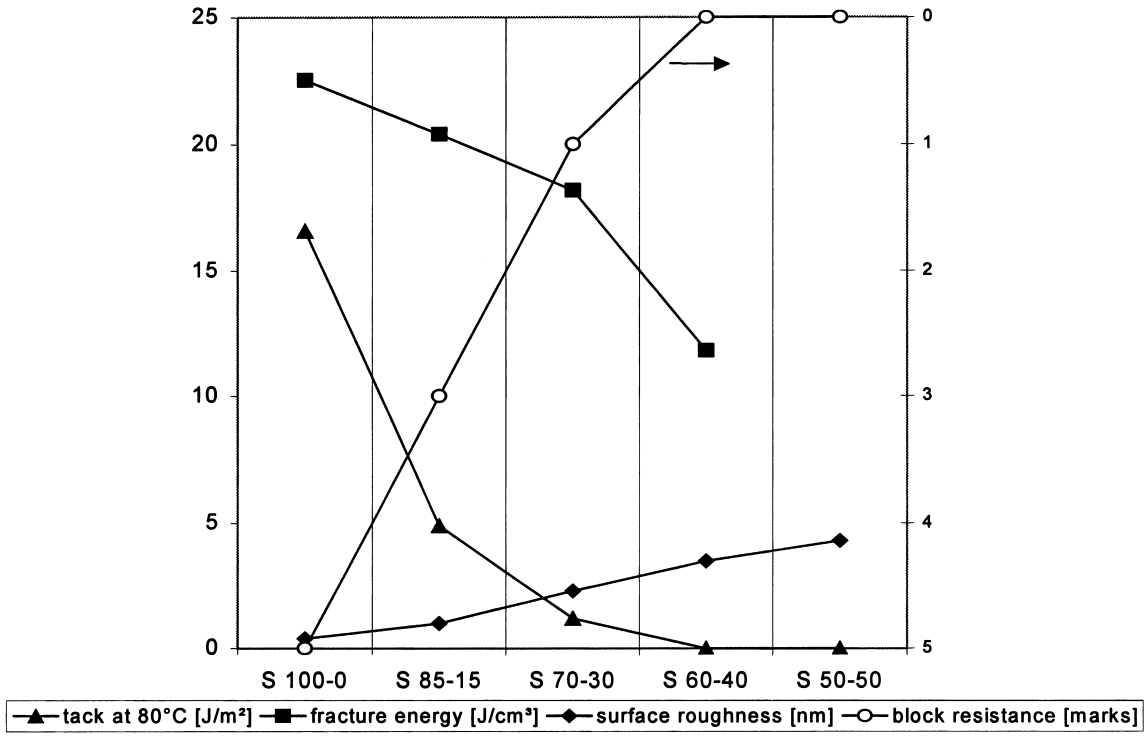

Fig. 6. Block resistance, tack, fracture energy and surface roughness of samples with different soft/hard ratios.

deformed but not ruptured. Thus, the fracture energy is a suited measure for the internal strength of the polymer film.

According to Table 6, the fracture energy E_f of the polymer films decreases with a higher hard/soft phase ratio. The reinforcement through the hard filler leading to improved tensile strength is overcompensated by the strong reduction of the elongation at break. Obviously, the increasing block resistance cannot be attributed to higher film cohesion.

In conclusion, the results demonstrate (Fig. 6) that the improvement of the block resistance by increasing the hard/soft ratio first of all is a consequence of the reduced adherence of the interfaces determined by the tack measurement. This is due to the increase of the amount of the hard phase material at the interface. The number of soft mobile polymer chains decreases which are able to interdiffuse and form a physical connection between the polymer films. A second reason might be the increasing roughness of the polymer surface as a result of the growing size of the hard particles sticking out of the soft matrix. The fracture energy or toughness of the polymer film plays no role in the block behavior.

To summarize, the properties of the dispersion film can clearly be attributed to the film morphology, which itself is determined by the structure of the single particles.

3.3. Paint film

In this section, paints formulated with the dispersions of the S-series are subjected to application testing. It is the last link in the chain to prove that the structure of the multiphase particles governs the properties of the corresponding paint film.

A simple recipe for an emulsion gloss paint was chosen (Table 7). It represents a low VOC formula to demonstrate the advantages of the multiphase particles in environment-friendly coatings.

The emulsion gloss paint, made of dispersions up to 35% hard phase, formed neat paint films without using any solvent. The S 60–40 paint could still be forced to form a film by the addition of 10% coalescent (butyl diglycol (BDG)), but in the case of S 50–50 and S 40–60 even higher amounts of BDG (30%) only led to a brittle film. These findings are in perfect agreement with the structure of the particles and the latex film, respectively. Starting from 50% hard phase share, the soft phase is completely engulfed. Thus, even if the amount of the coalescent was sufficient to reduce the MFFT of the hard PMMA-phase to or below room temperature, the continuous polymer phase of the resulting paint film would be composed of PMMA yielding a brittle coating.

Table 7
Recipe for the emulsion gloss paint employed[a]

20.0 pbw	Water
1.5 pbw	Agitan E 255 (defoamer)
10.0 pbw	Pigment dispersant MD 20
120 pbw	Rheolate 208 (5% solution) (thickener)
230 pbw	Kronos 2063 S (TiO_2 pigment)
589 pbw	Dispersion (45% solids content)
29.5 pbw	Water

[a] PVC: 19%; solids content: 50%.

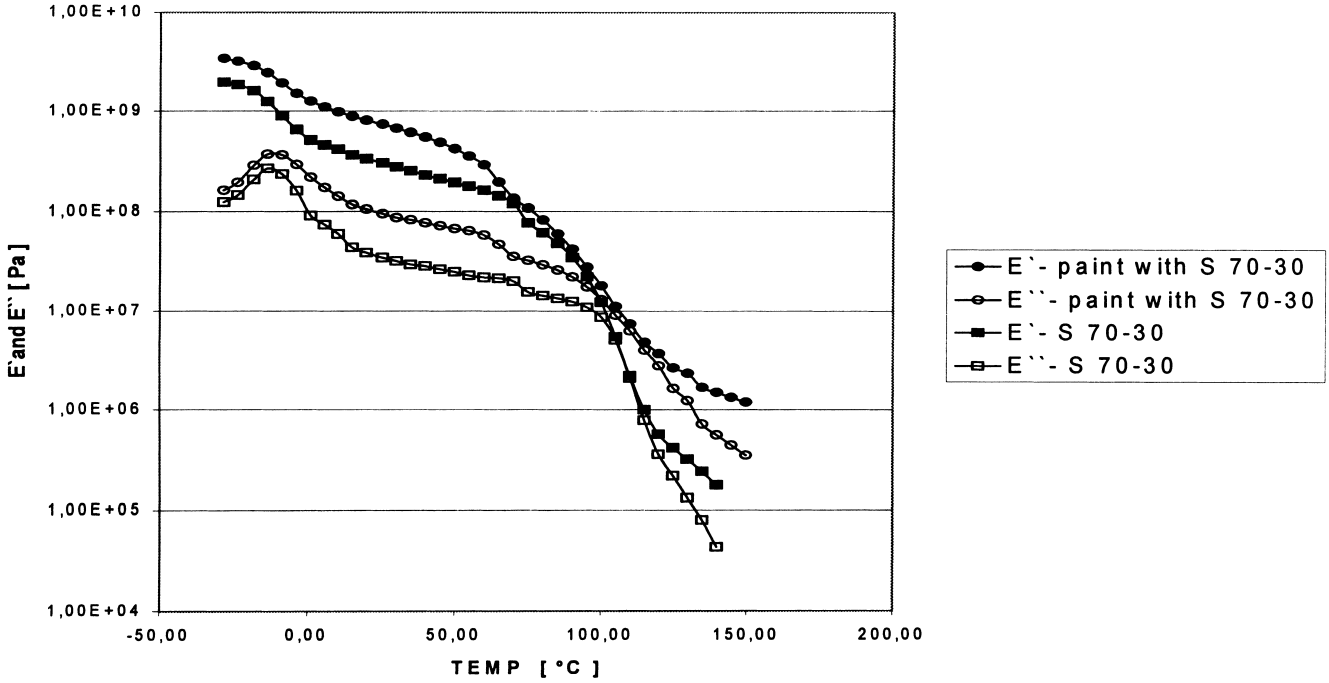

Fig. 7. $E'$and E''-moduli vs. temperature for the formulated paint with S 70–30.

Table 8
Tensile strength σ_B, elongation ε_B at break and fracture energy E_f for selected paint samples

Sample	σ_B (MPa)	ε_B (%)	E_f (J/cm^3)
S 100–0	1.3	1045	14.6
S 85–15	4.8	338	14.5
S 70–30	4.9	183	10.3

As proved by AFM, the morphology of the pure latex film is preserved in the paint film (Fig. 2). The mechanical properties of selected samples were examined. Fig. 7 demonstrates the change in the E' and E''-moduli through the transition from the latex film to the paint film. The TiO_2 pigment acts as an additional nonfilm-forming species, merely shifting both curves to higher level. As expected, the T_g of the polymer phases are left unchanged because of the incompatibility of the pigment and the polymer. The change in the moduli is also reflected in the stress/strain behavior (Table 8). The tensile strength increases and the elongation reduces if compared to the pure latex film (Table 6). The fracture energy is lowered by the transition from the S 100–0 latex film to the corresponding paint film due to the presence of the pigment. As expected, it further decreases with the additional incorporation of the hard polymer phase. The main application properties of the emulsion gloss paints are summarized in Table 9.

The dependence of the properties on the hard/soft phase ratio already found in the pure polymer film also shows up in the paint film. The block resistance estimated at 50 and 80°C improves with a higher hard/soft ratio as well as the pendulum hardness. The 60°-gloss stays on a high and constant

Table 9
Main application properties of the emulsion gloss paints

Sample	Block resistance[a]	Block resistance[b]	Pendulum hardness[c] (s)	Gloss[d] (20°/60°)
S 100–0	3	5	7	56/85
S 85–15	1	5	15	50/81
S 75–25	1	4–5	22	49/82
S 70–30	0	4	29	47/81
S 65–35	0	3	42	49/81
S 60–40[e]	0	3	49	36/72
S 50–50	No film formation			

[a] 200 μm wet on Leneta, 24 h drying time, contact area: 4 cm × 4 cm, 50°C/24 h/400 g/cm^2.
[b] 400 μm wet on wood, 24 h drying time, contact area: 4 cm × 4 cm, 80°C/24 h/400 g/cm^2.
[c] 240 μm wet, 14 h drying time, according to DIN 53157.
[d] 240 μm wet, 3 days drying time, measured with a Byk Gardener Micro-TRI-Gloss meter.
[e] Paint formulated with additional 10% BDG.

level. The 20°-gloss gradually decreases with an increasing amount of the hard phase material, probably due to the film-forming ability becoming worse. The results prove that multiphase particles allow the formulation of solvent-free emulsion gloss paints with a low MFFT as well as high hardness, good block resistance and high gloss by choosing the right morphology of the latex. The best combination of application properties could be achieved with 25–35% of the hard phase material.

4. Conclusion

Architectural coatings are increasingly required to fulfill demands for improved environmental compatibility. As a consequence, not only a shift from solvent-based to water-based dispersion paints has taken place, but also the demand is growing to completely abandon any volatile compound in the formulations. Especially, aqueous dispersion binders used in low-pigmented paint formulations, where the properties of the latex film play a major role, have to cope with the challenge to simultaneously show an excellent film formation and appearance as well as good block resistance and hardness without the addition of a coalescent. One strategy to overcome the contradictory requirements is the employment of multiphase particles.

In this work, it was proved that the structure of latex particles, synthesized by a two-stage emulsion polymerization process, can be correlated to the morphology and properties of the dispersion films as well as to the application properties of the corresponding paint films.

Two sets of model dispersions were made. In the first set, the hard/soft ratio was varied from 100% soft phase to 100% hard phase, and in the second set the amount of the AA was altered. The structure of the particles was determined by TEM and a morphology map was derived. AFM demonstrated a clear correlation between the particle structure and the morphology of the latex film. Dynamic mechanical analyses verified the presence of two distinct polymers, the hard phase acting as a transparent filler. For the hard/soft series, the properties of the dispersion films like block resistance, gloss and hardness could be attributed to their structure. A closer look on the block behavior revealed that it can be related to the tack and surface roughness of the dispersion film, but not to its internal strength. Solvent free emulsion gloss paints were formulated and application tests performed. The properties of the paint films correlated very well with those of the dispersion films. The test results clearly show that dispersions of multiphase particles enable the formulation of solvent-free paints with excellent film-forming ability in combination with high block resistance, hardness and gloss. The morphology of the latex particle thus determines the properties of the paint formulated therewith. Therefore, through the control of the thermodynamic and kinetic parameters that influence particle morphology, dispersions can be tailored for the desired application.

Acknowledgements

The authors want to thank Prof. El-Aasser and Mrs. Olga Shaffer, Lehigh University, Bethlehem, USA, for the collaboration in the electron microscopy studies.

References

[1] A.D. Broek, Prog. Org. Coat. 22 (1993) 55.
[2] H. Rinno, Farbe + Lack 99 (8) (1993) 697.
[3] H. De Hek, K.H. Zabel, P.J.A. Geurink, Surf. Coat. Aust. 35 (1998) 14.
[4] H.-C. Krempels, Farbe + Lack 100 (1) (1994) 13.
[5] M.A. Winnik, J. Feng, J. Coat. Technol. 68 (852) (1996) 41.
[6] S.T. Eckersley, B.J. Helmer, J. Coat. Technol. 69 (864) (1997) 97.
[7] Y. Chevalier, M. Hidalgo, J.-Y. Cavaillé, B. Cabane, ACS-Symposium Series 648, 1996, Chapter 16, p. 244.
[8] T.I. Min, A. Klein, M.S. El-Aasser, J.W. Vanderhoff, Polym. Sci., J. Polym. Chem. Ed. 21 (1983) 147.
[9] D.I. Lee, Makromol. Chem., Macromol. Symp. 33 (1990) 117.
[10] S. Torza, S. Mason, J. Colloid Interface Sci. 33 (1970) 67.
[11] J. Berg, D. Sundberg, B. Kronberg, Poly. Mat. Sci. Eng. 54 (1986) 367.
[12] D. Sundberg, A.P. Casassa, J. Pantazopoulos, M.R. Muscato, B. Kronberg, J. Berg, J. Appl. Polym. Sci. 45 (1990) 1425.
[13] Y. Chen, V. Dimonie, M.S. El-Aasser, Pure Appl. Chem. 64 (11) (1992) 1691.
[14] S. Lee, A. Rudin, ACS-Symposium Series 492, 1992, Chapter 15, p. 234.
[15] A. Rudin, Macromol. Symp. 92 (1995) 53.
[16] M. Okubo, Makromol. Chem., Macromol. Symp. 35/36 (1990) 307.
[17] I. Cho, K.W. Lee, J. Appl. Polym. Sci. 30 (1985) 1903.
[18] C.L. Zhao, J. Roser, W. Heckmann, A. Zosel, E. Wistuba, in: Proceedings of the 24th International Conference in Organic Coatings, 1998, p. 503.
[19] C.L. Winzor, D.C. Sundberg, Polymer 33 (18) (1992) 3797.
[20] Q. Zhong, D. Innis, K. Kjoller, V.B. Elings, Surf. Sci. 290 (1993) L688.
[21] A. Zosel, J. Adhesion 30 (1989) 135.
[22] V.L. Dimonie, E.S. Daniels, O.L. Shaffer, M.S. El-Aasser, in: P.A. Lovell, M.S. El-Aasser (Eds.), Emulsion Polymerization and Emulsion Polymer, Wiley, Chiston, Chapter 9.
[23] H.J. Sue, E.I. Garcia-Meitin, B.L. Burton, C.C. Garrison, J. Polym. Sci., Part B: Polym. Phys. 29 (1991) 1623.
[24] A. Zosel, W. Heckmann, G. Ley, W. Mächtle, Makromol. Chem., Macromol. Symp. 35/36 (1990) 423.
[25] T.G. Fox, Bull. Am. Phys. Soc. 1 (1956) 123.
[26] Tentative Method of Test for Peel Resistance of Adhesives, ASTM D1876-61T.
[27] D. Satas, Peel, in: Handbook of Pressure Sensitive Adhesive Technology, 2nd Edition, van Nostrand Reinhold, 1989.
[28] Standard Terminology of Adhesives, ASTM D907-82, 1985.
[29] M.P.J. Heuts, R.A. le Febre, J.L.M. van Hilst, G.C. Overbeek, ACS-Symposium Series 648, 1996, Chapter 18, p. 271.
[30] Standard Test Method for Holding Power of Pressure Sensitive Tapes, ASTM D3654-78.
[31] Z. Gao, H. Tsuo, J. Polym. Sci., Part B: Polym. Phys. 37 (1999) 155.